



ELSEVIER

Journal of Nuclear Materials 258–263 (1998) 634–639

Journal of
nuclear
materials

Material damage to beryllium, carbon, and tungsten under severe thermal shocks

J. Linke^{a,*}, R. Duwe^a, A. Gervash^b, R.H. Qian^a, M. Rödiger^a, A. Schuster^a

^a Forschungszentrum Jülich, EURATOM Association, D-52425 Jülich, Germany

^b D.V. Efremov Institute, St. Petersburg, 189 631, Russian Federation

Abstract

Material damage and erosion of plasma facing material and components due to severe thermal shocks which occur during disruptions and vertical displacement events have been investigated experimentally using electron beam devices. The deposited energy densities were $\leq 12 \text{ MJ m}^{-2}$ (disruption simulation) and 60 MJ m^{-2} (VDE simulation); effective pulse durations were 5 ms and 1 s, respectively. The resulting material degradation was determined by weight loss measurements, profilometry, metallography and scanning electron microscopy. © 1998 Elsevier Science B.V. All rights reserved.

1. Introduction

Plasma facing components in ITER will be subjected to severe thermal shocks during off-normal plasma operation scenarios [1]. Beside vertical displacement events (VDE) which occur on a relatively long time scale (0.1–1 s), plasma disruptions (on a millisecond time scale) are considered the most serious incidents. Under these conditions the plasma facing materials will be subjected to melting and/or evaporation processes thus forming a dense vapor cloud in front of the loaded component which will absorb a non-negligible fraction of the incident energy density [2]. Hence, the vapor shielding effect may significantly increase the erosion lifetime of plasma facing components. Nevertheless, the transmitted energy will cause severe erosion: melt layer removal in the case of beryllium or tungsten and particle emission in the case of carbon based materials. Additional material damage such as recrystallization, grain growth, crack

formation and degradation of the bond layer has a significant impact on the lifetime of the components.

2. Experimental results

Electron beam tests have been performed to simulate the surface heat loads during disruptions and VDEs. Different candidate materials for plasma facing components of ITER such as beryllium, doped and undoped carbon fiber composites, and tungsten alloys have been investigated in the Jülich Divertor Test Facility in Hot Cells (JUDITH) [3,4]. This facility allows the generation of short electron beam pulses ($t \geq 1 \text{ ms}$) with power densities up to 15 GW m^{-2} on surface areas of $3 \times 3 \text{ mm}^2$ to $5 \times 5 \text{ mm}^2$. The simulation of VDEs has been performed with absorbed power densities of 60 MW m^{-2} and effective pulse durations of approx. 1 s; here the loaded area was $10 \times 10 \text{ mm}^2$ or $15 \times 15 \text{ mm}^2$. In addition, some of the disruption simulation experiments have been performed in other test facilities, e.g. in the plasma accelerator VIKA of the D.V. Efremov Institute.

2.1. Simulation of plasma disruptions

To allow a precise quantification of the material erosion all test specimens have been polished prior to

* Corresponding author. Tel.: +49 2461 61 3230; fax: +49 2461 61 3699; e-mail: j.linke@fz-juelich.de.

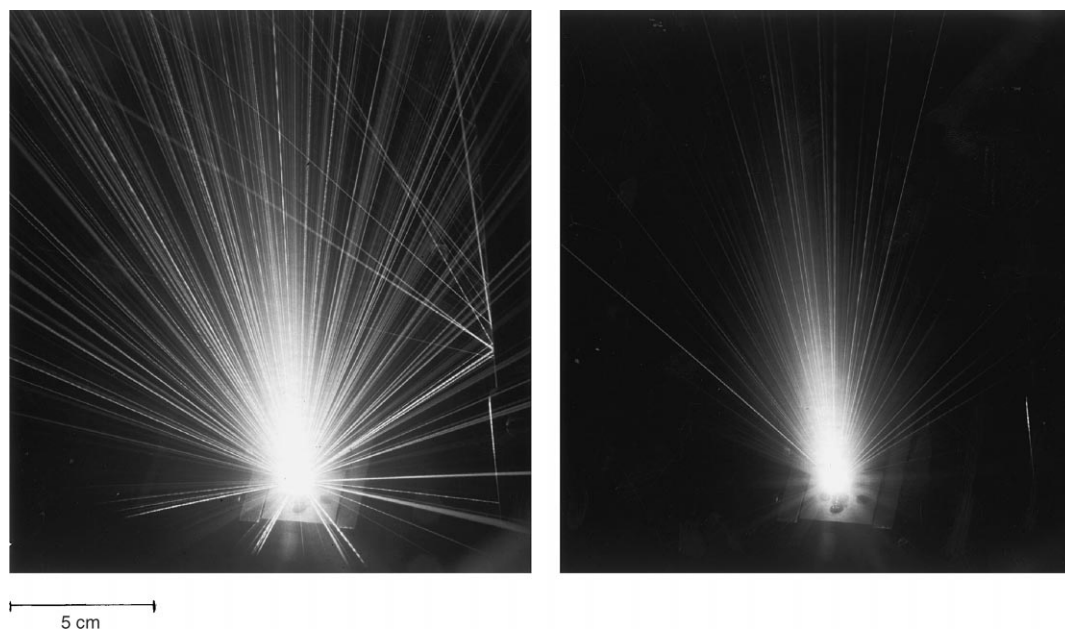


Fig. 1. Particle emission during electron beam loading of fine grain graphite (EK98) at 4.8 MJ m^{-2} , left: 1st electron beam pulse on a polished test sample, right: 5th electron beam pulse.

thermal shock loading to give them a well defined surface which is free from machining groves etc. Two- or three-dimensional surface profile measurements performed after electron beam loading give detailed results on volumetric changes, material erosion, or melt ejection from the crater [4]. In carbon-based materials the thermal erosion process is dominated by sublimation and particle ejection processes [5], which become effective at elevated temperatures, i.e. for $T \geq 1600\text{--}1700^\circ\text{C}$ [6]. The effect of particle emission is shown in Fig. 1 for graphitic test samples (EK98) which have been loaded repeatedly with intense electron beam pulses for 5 ms at 4.8 MJ m^{-2} . During the first pulse on the polished surface, the number of emitted particles is rather high. This results in a relatively high weight loss (and erosion depth). For subsequent electron beam pulses the number of emitted particles decreases; after 5–10 pulses the intensity remains constant.

Fig. 2 shows the time resolved measurements of the absorbed electrical current during electron beam loading for an incident beam current of 280 mA during the first, the second, and the fifth shot. A fraction (5–10%) of the incident current is reflected immediately. During the first pulse on the polished surface the absorbed current (approx. 260 mA) drops rapidly after about 2 ms to less than 100 mA, a process which is mainly associated with the emission of charged particles from the heated surface. This current decrease is retarded with increasing pulse number. In other words, a polished graphite sur-

face is rather sensitive to particle erosion. According to SEM micrographs it is primarily the graphitized binder which is eroded first; in the second step graphite grains or grain fragments which remain only loosely bound can be eroded easily. After a conditioning phase of approx. 5–10 shots the erosion per pulse remains constant. These findings are in good agreement with weight loss measurements which indicate that the most significant erosion takes place during the first electron beam shot [6].

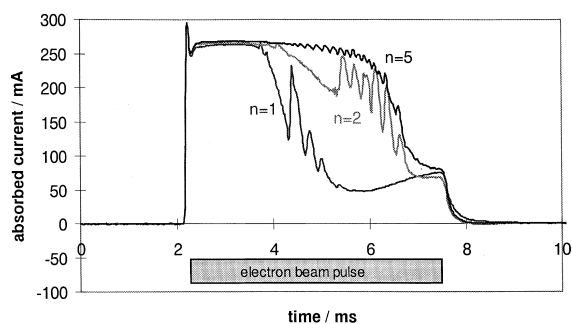


Fig. 2. Current absorbed by a graphitic test sample (EK98) during electron beam loading. Incident beam current: 280 mA, acceleration voltage: 120 keV, pulse duration: 5 ms. The three curves represent the 1st, 2nd and 5th shot.

The particle erosion process is associated with the emission of electrons (thermionic emission); in addition the release of charged particles from the heated surface (carbon clusters or grains) has been observed. In tokamaks these emission processes can lead to carbon blooms. According to the pyrometer measurements the emission process is becoming essential at surface temperatures of 1600–1700°C. In previous experiments using long pulse electron beam heating (1.5 s) [5] strong particle emission has been observed above approx. $T = 220^\circ\text{C}$.

Metallic test samples such as tungsten do not show any decreased current at identical loading conditions. Due to the formation of a liquid phase here the most critical erosion mechanism is associated with instabilities in the melt layer [7]. Plasma pressure, and may be gravitational forces may result in a rapid extraction of the melt layer. These effects have been studied in plasma accelerator experiments. Electron beam tests on metals have been performed to investigate the effect of thermal shock induced surface modifications.

Results on the HHF behavior of different beryllium grades have been reported elsewhere [4]. In general be-

ryllium exhibits little ductility; hence, a careful analysis of thermal shock induced cracks is inevitable. Refractory metals such as tungsten also behave brittle, at least when thermal shock loaded at temperatures below DBTT. Thus alloyed tungsten materials have been suggested as alternative candidates for high heat flux components. Among these were W5Re (with 5% rhenium alloyed W), WLa_2O_3 (W alloyed with 1% La_2O_3), W30Cu (W with 30% Cu) and plasma-sprayed tungsten. These materials have been exposed to 5 ms thermal shocks with deposited energy densities of up to 12 MJ m^{-2} . Compared to pure tungsten [8] the Re- and La_2O_3 -alloyed tungsten grades show a rather high tendency to form deep cracks perpendicular to the sample surface which are oriented parallel to each other, cf. Fig. 3. Some of these cracks which have been observed on all samples ($E_{\text{abs}} = 7\text{--}12 \text{ MJ m}^{-2}$) extend from the loaded surface to the back of the 5 mm thick specimens, shorter cracks penetrate to a depth of only less than 1 mm. Both materials (W5Re and WLa_2O_3) show a strong anisotropy in the grain morphology with a plate like grain shape; the orientation of the individual platelets was perpendicular to the specimen surface. The behavior

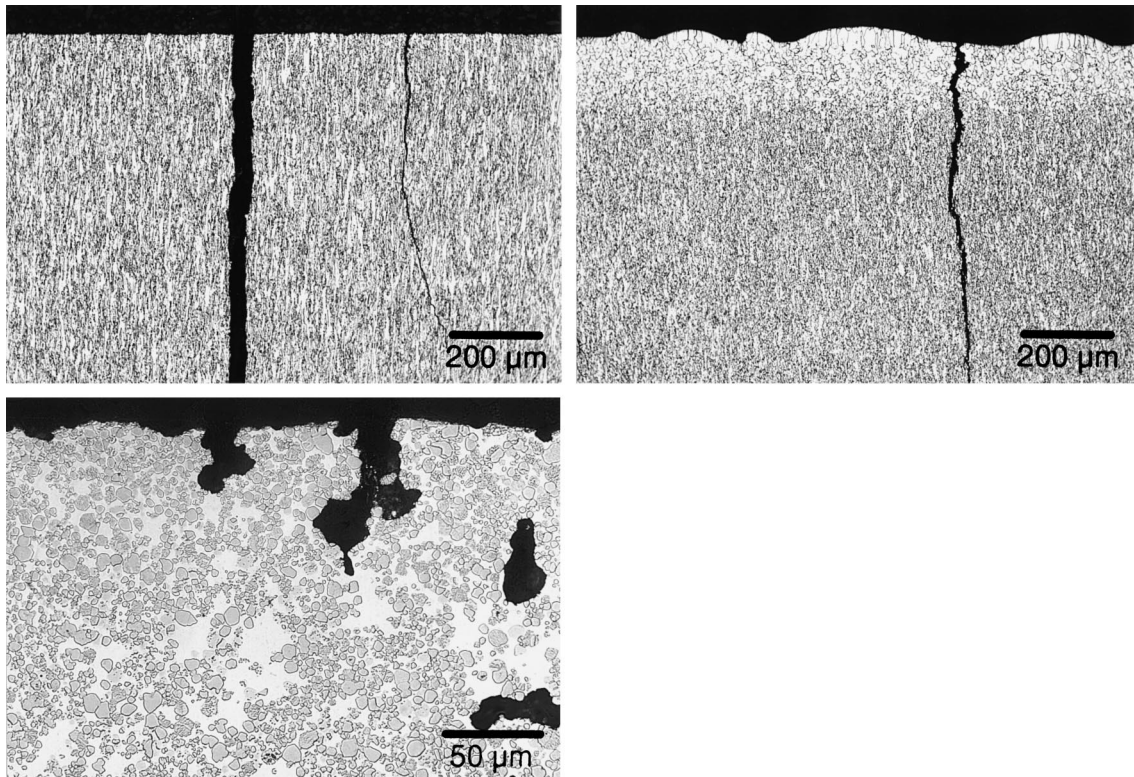


Fig. 3. Metallographic sections from different tungsten alloys loaded with five electron beam pulses ($E_{\text{abs}} = 11.8 \text{ MJ m}^{-2}$, $t = 5 \text{ ms}$). Left: W5Re; right: WLa_2O_3 ; lower left: W30Cu.

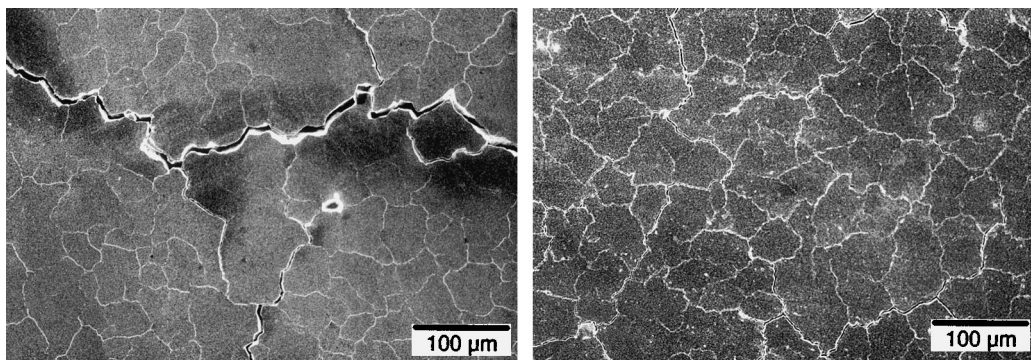


Fig. 4. Surface morphology from tungsten specimens loaded at incident energy densities of 7.5 MJ m^{-2} ($t = 360 \text{ } \mu\text{s}$) in VIKA. Left: $T_{\text{sample}} = 330^\circ\text{C}$, right: $T_{\text{sample}} = 640^\circ\text{C}$.

of W30Cu differs significantly; here almost no cracks have been generated at similar energy densities. However, due to the incident heat load part of the copper was molten and ejected or evaporated. The remaining open porosity extends to a depth of $400 \text{ } \mu\text{m}$.

To investigate the behavior of refractory metals at elevated temperatures, disruption simulation tests have been performed in the plasma accelerator VIKA [8] with a pulse duration of up to $360 \text{ } \mu\text{s}$. Fig. 4 shows the material response for pure tungsten at heat loads of 7.5 MJ m^{-2} . The sample temperatures were 330°C and 640°C , respectively. The lower temperature is below DBTT; i.e. the material still behaves brittle. Upon thermal shock loading intergranular cracks are generated; typical depth values are in the order of $30 \text{ } \mu\text{m}$. At 640°C , i.e. above DBTT, the surface crack density is reduced significantly. The main material damage in this temperature regime is a widening of the grain boundaries; the integrity of the bulk material remains greatly unaffected. At higher incident energy densities (30 MJ m^{-2}) additional melting of the tungsten occurs; the melt layer thickness is in the order of 150 to $200 \text{ } \mu\text{m}$. For low sample temperatures intense surface cracks have been observed in the recrystallized area; however, almost no cracks developed at temperatures above DBTT.

2.2. Simulation of vertical displacement events

Beside plasma disruptions VDEs have significant impact on the lifetime of plasma facing components [9]. VDEs occur on a much longer time scale (typically in the order of 0.1 – 1 s). Under these conditions the penetration depth of the heat front is not limited to the plasma facing material only; i.e. the bond layer will be heat affected too. Hence, experiments have been performed on miniaturized components consisting of beryllium or CFC armor bonded to an actively cooled copper heat sink. Be-tiles made from S65 C with a thickness of 3 and

6 mm , respectively, were brazed to a CuCrZr heat sink alloy by an induction brazing process with a CuMnSnCe braze. Similar tests have been performed on mock-ups using an InCuSil braze and on a HIPed module (DS-Cu substrate). VDE tests on CFC mock-ups of the monoblock design (Dunlop Concept1 brazed to CuCrZr, and SEPCARB N31 joined to a DS-copper tube) have been performed with identical armor thicknesses and load cycles. Since the energy supply system (transformer) does not allow fast transients at high beam currents, a loading cycle of 1.5 s was applied (0.5 s each for the ramp-up, for the full power and for the ramp-down phase). The applied heat flux at full power was 60 MW m^{-2} (this corresponds to a deposited energy density of 60 MJ m^{-2}).

Fig. 5 shows typical surfaces and metallographic cross sections parallel to the coolant tube of a beryllium and a CFC armored mock-up after a single VDE simulation test. The beryllium tiles show severe melting. The metallographic sections show a rather homogeneous melt zone with a columnar grain structure; castellations are partially filled with resolidified beryllium. The resulting melt layer has a thickness of approx. $900 \text{ } \mu\text{m}$ for a Be thickness of 3 mm and $1500 \text{ } \mu\text{m}$ for the 6 mm armor. There are almost no cracks detectable, neither in the recrystallized zone, nor in the undamaged S65 C. Metallographic examinations from the braze joints do not indicate any defects. The HIPed joint (S65 C on DS-copper) however showed intense delamination at the interface, particularly at the corner of the mock-up.

Monoblock mock-ups with CFC armor did not show any visible damage at identical heat load scenarios. Beside some minor discoloration at the loaded surface the carbon fiber composite material (SEPCARB N31) has not been eroded; the braze joint remains intact. This is also true for the CONCEPT 1-CuCrZr mock-up, which has been loaded at 10 repeated VDE-cycles of 60 MJ m^{-2} each on the 3 and the 6 mm thick armor.

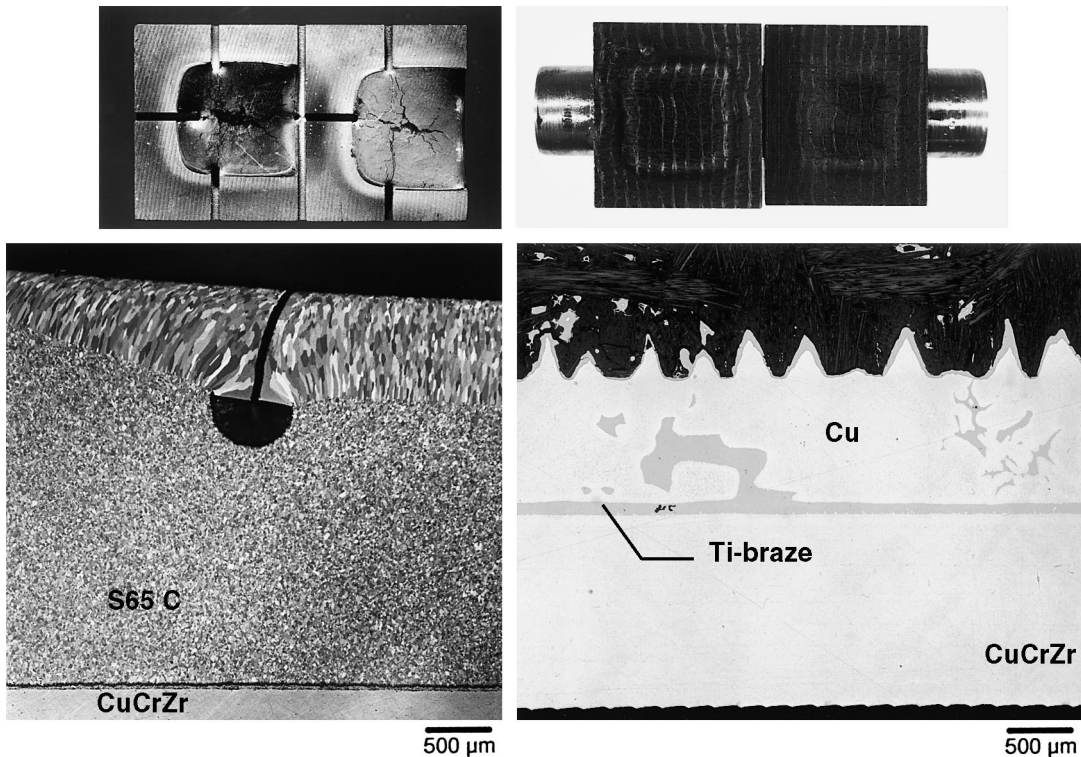


Fig. 5. Simulation of Vertical Displacement Events on mock-ups with beryllium (3 mm S65 C-InCuSil-braze-CuCrZr, left) and CFC armor (3 and 6 mm SEPCARB N31-Ti-braze-CuCrZr, right). The actively cooled modules have been loaded with energy densities of 60 MJ m^{-2} (effective pulse duration: 1 s).

3. Conclusions

Different candidate PFMs for ITER have been investigated under severe thermal shocks to simulate plasma disruptions. The major erosion mechanism for carbon based materials (CFCs, graphites) is by particle emission and sublimation. In low melting point metals such as beryllium, rather thick melt layers are generated; the risk of a complete melt layer loss is significant and will greatly affect the life time of the component. The melt layer in pure tungsten is less sensitive because of the higher melting point. Both for Be and W thermal shock induced crack formation is essential; however, this effect can be neglected at elevated temperatures ($T > \text{DBTT}$).

VDEs with energy densities of 60 MJ m^{-2} deposited during 1 s on CFC monoblock mock-ups do not affect the integrity of the components; erosion of the CFC material is negligible. Modules with Be armor however show severe melting. Bond layers with brazed joints (InCuSil or CuMnSnCe) remain intact; HIPed joints failed under identical thermal loads.

Acknowledgements

The authors would like to acknowledge the assistance of H. Klöcker, W. Kühnlein and H. Münstermann in the electron beam experiments. In addition V. Gutzeit and H. Hoven assisted in the metallographic examination.

References

- [1] R.R. Parker, Fusion Eng. Design 36 (1997) 33.
- [2] A. Hassanein, I. Konkashbaev, Fusion Technol. 1996, Elsevier Science (1997) 379.
- [3] R. Duwe, W. Kühnlein, H. Münstermann, Proceedings of the 18th Symposium on Fusion Technology, Karlsruhe, Aug. 1994, pp. 355–358.
- [4] M. Rödiger, R. Duwe, J. Linke, R.H. Qian, Proceedings of the 17th IEEE/NPSS Symposium on Fusion Engineering, San Diego, Oct. 1997.
- [5] J. Bohdansky et al., Nucl. Instr. and Meth. 23 (1987) 527.
- [6] J. Linke, M. Akiba, H. Bolt, G. Breitbach, R. Duwe, A. Makhankov, I. Ovchinnikov, M. Rödiger, E. Wallura, J. Nucl. Mater 241–243 (1997) 1210.

- [7] P. Schiller, F. Brossa, M. Cambini, D. Quataert, G. Rigon, Fusion Eng. Design 6 (1988) 131.
- [8] A. Gervash, E. Wallura, I. Ovchinnikov, A.N. Makhankov, J. Linke, G. Breitbach, Proceedings of the 19th Symposium on Fusion Technology, Lisbon, Sept. 1996, pp. 499–502.
- [9] M. Merola, M. Rödiger, J. Linke, R. Duwe, G. Vieider, these Proceedings.